

## Supplementary Information for

### **Gene expression in oligodendrocytes during remyelination reveals cholesterol homeostasis as a therapeutic target in multiple sclerosis**

Rhonda R. Voskuhl <sup>1\*</sup>, Noriko Itoh <sup>1</sup>, Alessia Tassoni <sup>1</sup>, Macy Akiyo Matsukawa <sup>1</sup>,  
Emily Ren <sup>1</sup>, Vincent Tse <sup>1</sup>, Ellis Jang <sup>1</sup>, Timothy Takazo Suen <sup>1</sup>, Yuichiro Itoh <sup>1</sup>

Corresponding author: Rhonda R. Voskuhl  
Email: [rvoskuhl@mednet.ucla.edu](mailto:rvoskuhl@mednet.ucla.edu)

#### **This PDF file includes:**

Supplemental Materials and Methods  
Figs. S1 to S10  
Tables S4 to S6  
Caption for Table S1, S2, S3  
References for SI

#### **Other supplementary materials for this manuscript include the following:**

Table S1 (Gene lists)  
Table S2 (Gene lists)  
Table S3 (Gene lists)

## **Supplementary Information Text**

### **Supplemental Materials and Methods**

#### **High throughput RNA sequencing analysis of tissues from MS**

Five female MS patients (average age = 57.6 years) and five female age-matched healthy controls (average age = 56.2 years) fresh frozen autopsy brain tissue samples were obtained from Human Brain and Spinal Fluid Research Center in Los Angeles. Regions included corpus callosum, optic chiasm, internal capsule, hippocampus, frontal cortex and parietal cortex. We requested tissues without lesions by neuropathology in order to examine gene expression in normal appearing white matter and normal appearing gray matter. MS types included 1 relapsing remitting with transition to SP, 3 progressive, 1 unknown; DMTs were not used in 4 and unknown in 1; History of optic neuritis was confirmed in 1, and unknown in 4. Tissues were homogenized into Trizol Reagent (Thermo Fisher Scientific), and aqueous phase was collected after phase separation by adding chloroform. Further RNA purification was performed using Direct-zol™ RNA MiniPrep Plus (Zymo Research). The RNA integrity numbers (RIN) were between 6.1-8.7 for MS (average 7.64) and 5.1-8.3 for normal control (average 7.1).

The RNA sequencing library was made using KAPA Stranded RNA-Seq Kit (Kapa Biosystems) which consists of mRNA enrichment, cDNA generation, end repair, A-tailing, adaptor ligation, strand selection, and PCR amplification. Barcoded adaptors were used for multiplexing samples in one lane. Sequencing was performed on Illumina HiSeq3000 for a single end 1x50 run. Data quality check was done on Illumina SAV. De-multiplexing was performed with Illumina

Bcl2fastq2 v 2.17 program. These procedures were performed in the UCLA Technology Center for Genomics and Bioinformatics.

Quality of raw sequence data were examined using FastQC (<http://www.bioinformatics.babraham.ac.uk/projects/fastqc/>), and Trimmomatic (1) was used for cleaning. R package “QuasR” (2) was used for the read alignment to human genome (hg19) followed by the counting at gene level. Differentially expressed genes between MS and healthy controls were identified using R package “edgeR” (3). False discovery rate of 0.1 was used as a threshold of differentially expressed genes. To estimate the differentially expressed gene numbers in various CNS cell types, lists of top 500 enriched genes in 7 CNS cell types (neuron, microglia, astrocyte, endothelia, OPC, newly formed oligodendrocyte, and myelinating oligodendrocyte) from the RNA-sequencing transcriptome database (4) were used as a reference gene list.

### **Animals.**

All mice used in this study were young adult females (age 8-12 weeks) on a C57BL/6 background. Olig1-RiboTag mice: B6;129S4-*Olig1*<sup>tm1</sup>(cre)Rth/J (Olig1-Cre) mice and B6N.129-*Rpl22*<sup>tm1.1</sup>*Psam*/J (RiboTag) mice were purchased from Jackson Laboratory (5, 6). The two transgenic mice were crossed to obtain homozygote mice of Olig1-cre and RiboTag (Olig1-RiboTag), expressing HA-tagged ribosomal protein RPL22 in Olig1<sup>+</sup> oligodendrocyte lineage cells. Olig1-CKO mice: C57BL/6J-ER $\beta$ <sup>floxed/floxed</sup> mice (7) were crossed with B6;129S4-*Olig1*<sup>tm1</sup>(cre)Rth/J (Olig1-cre) mice to obtain mice with ER $\beta$  selectively deleted

in Olig1<sup>+</sup> oligodendrocyte lineage cells. *Cspg4-CreERT2/Mapt-GFP* mice: B6.Cg-Tg(*Cspg4-cre/Esr1\**)BAKik/J and B6;129P2-Mapt<sup>tm2Arbr</sup>/J were also purchased from Jackson Laboratory. The two transgenic mice were crossed to obtain a mouse line allowing lineage-specific tracing of remyelination by newly formed oligodendrocytes (8). Animals were maintained under standard conditions in a 12 h dark/12 h light cycle with access to food and water ad libitum. All procedures were done in accordance to the guidelines of the National Institutes of Health and the Chancellor's Animal Research Committee of the University of California, Los Angeles Office for the Protection of Research Subjects.

#### **Cuprizone model.**

Young adult female mice (age 8-10 weeks) were fed with 0.2% bis-(cyclohexanone)-oxaldihydrazone (cuprizone) diet (TD.140803, Harlan Teklad) for 6 weeks or 9 weeks to induce demyelination, followed by a 3 week recovery period on global 18% protein rodent control diet (TD.00588, Harlan Teklad) to induce natural remyelination. For ER $\beta$ -ligand treatment we used diarylpropionitrile (DPN, Tocris) as described (7). DPN was first dissolved in 100% ethanol and then diluted at 1:9 ration in 100% Miglyol®812 (CREMER Oleo GmbH & Co. KG), reducing the final ethanol concentration to 10%. ER $\beta$ -ligand treatment was given during the 3 week normal diet period through subcutaneous injections every other day at a dose of 8 mg/kg per day until the end of the experiment. For randomization, after cuprizone diet feeding, mice were randomly assigned to treatment with vehicle or ER $\beta$ -ligand for 3 weeks

while on normal diet. For blinding of drug treatment, third party concealment with color coded labeling of vehicle or ER $\beta$ -ligand treatment syringes was done before treatment started for each experiment.

### **Experimental autoimmune encephalomyelitis model and ER $\beta$ -ligand treatment**

Female mice (age 8-12 weeks) were immunized subcutaneously with myelin oligodendrocyte glycoprotein (MOG), amino acids 35–55 (200  $\mu$ g per mouse, Mimotopes) emulsified in Complete Freund's Adjuvant, supplemented with *Mycobacterium Tuberculosis* H37Ra (200  $\mu$ g per mouse, Difco Laboratories), over two sites drained by left inguinal and auxiliary lymph nodes in a total volume of 0.1 ml per mouse (Day 0). Pertussis toxin (500 ng per mouse, List Biological Laboratories) was injected intraperitoneally on Day 0 and Day 2. On Day 7, a booster immunization was delivered over contralateral lymph nodes. The animals were monitored daily for EAE signs based on a standard EAE 0–5 scale scoring system: 0, healthy; 1, complete loss of tail tonicity; 2, loss of righting reflex; 3, partial paralysis; 4, complete paralysis of one or both hind limbs; and 5, moribund (9). ER $\beta$ -ligand treatment was initiated 1 week before EAE induction and given through subcutaneous injections every other day at a dose of 8 mg/kg per day until the end of the experiment. ER $\beta$ -ligand treatment preparation and randomization were done using the same method mentioned above. For *Cspg4-CreERT2/Mapt-GFP* transgenic mice, Tamoxifen (Sigma-

Aldrich, St. Louis, MO) was dissolved in corn oil (75 mg/kg) and administered subcutaneously two weeks prior ER $\beta$ -ligand treatment for 5 consecutive days.

### **Ovariectomy**

To eliminate the effects of circulating endogenous estrogens during the experiments, ovariectomy was performed in female mice (age - 5 weeks). Mice were anesthetized by inhalational anesthesia with isoflurane. Carprofen (1.2 mg/ml per animal, Zoetis) and 0.5 ml of saline were injected subcutaneously before the procedure. The fur above the lateral dorsal back was removed, and the skin was sterilized with betadine and alcohol scrubs. Bilateral incisions were made into the back. A hemostat was placed on the fallopian tubes, and the ovaries were removed. Muscle layer was closed with absorbable suture, and the skin layer was closed with wound clips. Amoxicillin (50 mg/ml, Virbac) was added to the water for 5 days for antibiotics (0.5 mg/ml water), and another dose of carprofen was given within 24 h following surgery. Wound clips were removed 7 days later as described (7). All procedures were approved by the Office of Animal Research Oversight and UCLA institutional animal care and use committee, known locally as the Chancellor's Animal Research Committee.

### **High throughput RNA sequencing of oligodendrocytes during remyelination.**

Mice were exposed to a lethal dose of isoflurane and transcardially perfused with ice-cold 1xPBS for 4 min, followed by perfusion with ice-cold 1%

paraformaldehyde-1xPBS for 4 min. Corpus callosum, spinal cord, and optic nerve tissues were collected, snap-frozen in liquid nitrogen and stored at -80°C. Frozen tissues were homogenized on ice using the Dounce Homogenizer with freshly made homogenization buffer containing: 50mM Tris-HCl (Invitrogen) pH 7.5, 100mM KCl (Fisher scientific), 12mM MgCl<sub>2</sub> (Fisher Scientific), 1% Nonidet P-40 (Roche), 1mM DTT (Sigma-Aldrich), 1x Proteinase Inhibitors (Sigma-Aldrich), 200 units/ml RNAsin (Promega), 100ug/ml cycloheximide (Sigma-Aldrich), and 1mg/ml heparin (Sigma-Aldrich). The homogenates were then centrifuged at 16,000xg, 4 °C for 15 min. The supernatant was collected and incubated with pre-washed anti-HA conjugated magnetic beads (Pierce) overnight on a rotating wheel at 4 °C. After removal of the supernatant, the magnetic beads were washed 3 times with high salt buffer containing: 50 mM Tris (pH 7.5), 300 mM KCl, 12 mM MgCl<sub>2</sub>, 1% Nonidet P-40, 1 mM DTT, 100 g/ml cycloheximide. Then, 25 µl of proteinase K (4 mg/ml; Zymo Research) was added to the samples and incubated in a 55°C water bath for 30 minutes. After incubation, 300 µl Tri-reagent was added, and the Direct-zol™ RNA MiniPrep Plus kit (Zymo Research) was used for RNA isolation according to manufacturer's instructions. RNA quantity and quality were measured using NanoDrop 2000 spectrophotometer (Thermo Scientific) and Agilent 2100 Bioanalyzer with pico chip, respectively as described (9).

The RNA sequencing library was made using KAPA Stranded RNA-Seq Kit (Kapa Biosystems) which consists of mRNA enrichment, cDNA generation, end repair, A-tailing, adaptor ligation, strand selection, and PCR amplification.

Barcoded adaptors were used for multiplexing samples in one lane. Sequencing was performed on Illumina HiSeq3000 for a single end 1x50 run. Data quality check was done on Illumina SAV. De-multiplexing was performed with Illumina Bcl2fastq2 v 2.17 program. These procedures were performed in the UCLA Technology Center for Genomics and Bioinformatics.

Statistical analyses and production of figures were performed in R (R Core Team, 2018, <http://www.R-project.org/>). Qualities of raw sequence data were examined using FastQC (<http://www.bioinformatics.babraham.ac.uk/projects/fastqc/>), and Trimmomatic was used for cleaning. R package “QuasR” was used for the read alignment to the mouse genome (mm10) followed by the counting at the gene level. To visualize the relationship of samples, the principal component analysis was performed. We assumed read counts followed a negative binomial distribution and constructed generalized linear models based on this negative binomial distribution assumption. Genes differentially expressed between control (Normal) mice receiving cuprizone diet for 9 weeks (9w) versus mice receiving cuprizone diet for 9 weeks followed by normal diet for 3 weeks (9w+3w) were identified using R package “edgeR.” False discovery rate (FDR) of 0.1 was used as a threshold of differentially expressed genes, as described (9, 10). Canonical pathway enrichment analysis was performed for differentially expressed genes in each tissue using Ingenuity Pathway Analysis (QIAGEN, Redwood City, [www.qiagen.com/ingenuity](http://www.qiagen.com/ingenuity)) as described (9).



### **Quantitative RT-PCR (qPCR)**

cDNA was synthesized using the Tetro cDNA Synthesis kit (Bioline) according to manufacturer's instructions. qPCR was performed using PowerUp™ SYBR™ Green Master Mix (Thermo Fisher Scientific) on the Bio-Rad Opticon 2 qPCR / Peltier Thermal Cycler. See Table S5 for primer information. The efficiency of each set of primers was assessed by qPCR on a serial dilution of cDNA from CNS tissues and was confirmed to be above 90%. All gene expression levels were normalized to the levels of  $\beta$ -actin by using the standard curve method and expressed as fold change.

### **Histological preparation**

Mice were exposed to a lethal dose of isoflurane and perfused transcardially with ice-cold 1xPBS for 8 min, followed by 10% buffered formalin for 8 min. Brains, spinal cords and optic nerves were dissected and stored in 10% buffered formalin overnight at 4°C, then submerged in 30% sucrose, 0.1% sodium azide, 1xPBS for 24 h at 4°C. Tissues were embedded in optical cutting temperature compound (OCT, Tissue Tek) and stored at -80°C after flash freezing in an isopropanol bath chilled with liquid nitrogen. Tissues were cryosectioned at -25°C into 40  $\mu$ m thick (brain and spinal cord) and 10  $\mu$ m thick (optic nerve) sections using a cryostat (Leica CM1860) and stored in 0.1% sodium azide, 1xPBS at 4°C before used for immunofluorescence staining.

### **Immunofluorescence staining**

Brain (between bregma -2 to 0), spinal cord (thoracic region) and optic nerve sections were washed thoroughly using 1xPBS with 0.1% TritonX-100 (PBSt). Tissue sections were incubated with 5% glacial acetic acid, 95% ethanol solution for 30 min at room temperature (RT) and then washed with 1xPBSt before blocking. For blocking, tissues were treated with 10% normal goat serum (NGS) in 1xPBSt for 1 hour at RT. Primary and secondary antibody stainings were done at appropriate concentrations with 2% NGS, 1xPBSt for overnight at 4°C and 1 hour at RT, respectively. Nuclei were stained with DAPI at 1:5000 concentrations in 1xPBS. After serial washes, sections were mounted onto slides (Superfrost®Plus, VWR), allowed to semi-dry, and coverslipped (24x60, Fisher Scientific) with fluoromount®G (SouthernBiotech) for confocal microscopy as described (7). List of antibodies are provided in Table S6.

### **Confocal microscopy and analysis**

Stained sections were examined and imaged using Olympus BX51 fluorescence microscope with a DP50 digital camera. Images were taken in stacks, 10x images were taken at 8-10 µm thickness with 2 µm stacks and 40x images were taken at 5-6 µm thickness with 1 µm stacks. All images were taken and processed using the integrated software program Slidebook4.2 (Intelligent Imaging Innovations). ImageJ (NIH) was used to perform integration and analysis of images. All analyses were done in a blinded fashion with regards to knowledge of treatment randomization as described (7).

## **Electron microscopy and analysis**

Mice were exposed to a lethal dose of isoflurane and perfused transcardially with ice-cold 1xPBS for 8 min, followed by 2.5% glutaraldehyde, 2% paraformaldehyde in 0.1M phosphate buffer, 0.9% sodium chloride for 8 min. Corpus callosum region of the brain and thoracic portions of the spinal cords were dissected and post fixed for 2 hours at room temperature in the same fixative and stored at 4°C until processing. Tissues were washed with 1xPBS, post fixed in 1% OsO<sub>4</sub> in ddH<sub>2</sub>O for 90 minutes on ice, dehydrated in a graded series of ethanol, treated with propylene oxide and infiltrated with resin Eponate 12 (Ted Pella) overnight. Tissues were embedded in fresh Eponate and polymerized at 60°C for 48 hours. Approximately 50-60 nm thick sections were cut on an RMC MT-X ultramicrotome and picked up on formvar coated copper grids. The sections were stained with uranyl acetate and lead citrate and examined on a JEOL 100CX electron microscope at 60kV. Images were collected on type 4489 EM film, and the negatives scanned to create digital files. Films (Kodak) were developed and scanned at high resolution. The analysis was done with ImageJ and g-ratio was used for the extent of remyelination on axons.  $g\text{-ratio} = (\text{axon diameter}) / (\text{axon} + \text{outer myelin diameter})$  as described (7).

## **ER $\beta$ CHIP-Seq profiles for cholesterol synthesis genes.**

CHIP-Seq data for doxycycline-inducible ER $\beta$  expressing human MDA-MB-231 cells treated with estradiol was obtained from GEO (GSE108981) (11). Briefly, cells were treated with 100 ng/ml doxycycline to induce ER $\beta$  expression,

treated with 1 nM estradiol for 3 hours, then ChIP-Seq was performed. R package “QuasR” (2) was used for the alignment to human genome (hg19), and ER $\beta$  binding profiles were generated with input from R package “GenomicFeatures” (12) and “Gviz” (13). The profiles for ER $\beta$  ChIP, as well as input negative control (DNAs from chromatin before ChIP), were each analyzed for cholesterol genes.

### **ChIP assay to assess ER $\beta$ binding to estrogen response element of *Fdps***

The immortalized Mouse N20.1 oligodendrocytic cell line(14) was a gift from Dr. Paez's laboratory (Hunter James Kelly Research Institute, University at Buffalo). N20.1 cells were grown in DMEM/F-12/HEPES/no phenol red medium (Thermo Fisher Scientific) supplemented with 100  $\mu$ g/ml G418 and 10% charcoal stripped fetal bovine serum (Gibco). When the confluency reached about 50-60%, DPN was added to the medium at 10nM. This treatment was repeated for 3 days. Before harvesting the cells, cells were treated with DPN for 30 minutes to enhance the DNA binding of ER $\beta$  protein. Chromatin immunoprecipitation was performed using EZ-Magna ChIP™ A/G (Millipore) with ER beta/NR3A2 Antibody (Novus Biologicals) and normal mouse IgG (incorporated in EZ-Magna ChIP™ A/G kit). Immunoprecipitated DNAs around putative ERE of *Fdps* gene (AGGTCAACTTGACAC)(15) were amplified by PCR using the primer set 1 (5'-TCCCTCTTCTCCAAAGCATC-3', 5'- AATCTGGTGTGCGCATT TTT-3') and primer set 2 (5'- TCATGTGGCTCCCTCTTCTC-3', 5'-TTGAGAGTCCCTCTTTCCAA-3').

## **Statistical analyses**

Statistical analyses of immunofluorescence experiments to establish the optimal time course of the chronic cuprizone model were evaluated using one-way ANOVA with Bonferroni's multiple comparison tests. Statistical analyses of qPCR results were evaluated using unpaired two-tailed t-tests (Student's t-tests) or one-way ANOVA with Bonferroni's multiple comparison tests. Statistical analyses of immunofluorescence experiments for validation of cholesterol synthesis gene expression were evaluated using unpaired two-tailed t-tests (Student's t-tests). Statistical analyses of immunofluorescence experiments in ER $\beta$ -ligand treatment studies in the cuprizone model were evaluated using two-way ANOVA with Bonferroni's multiple comparison tests for comparing treatment effects in two different transgenic groups, and one-way ANOVA with Bonferroni's multiple comparison tests for normal controls or chronic demyelination (9w) versus other groups. Regarding EAE, repeated measures two-way ANOVA, with Bonferroni's multiple comparisons test, were used. Data are presented as means  $\pm$  S.E.M. Power calculations for the experiments were determined for sample size to reach  $P < 0.05$  by Myung S. Sim, M.S. Dr.PH, in the Department of Medicine Statistic Core at UCLA. A minimum of 4-5 animals per group was stated to provide statistical significance at a level of  $P < 0.05$  using 95% power analysis, consistent with numbers used in the field. All statistical analyses were performed using Prism 6 (version 6.01) software (GraphPad, CA) unless otherwise stated.

## Supplemental Figures

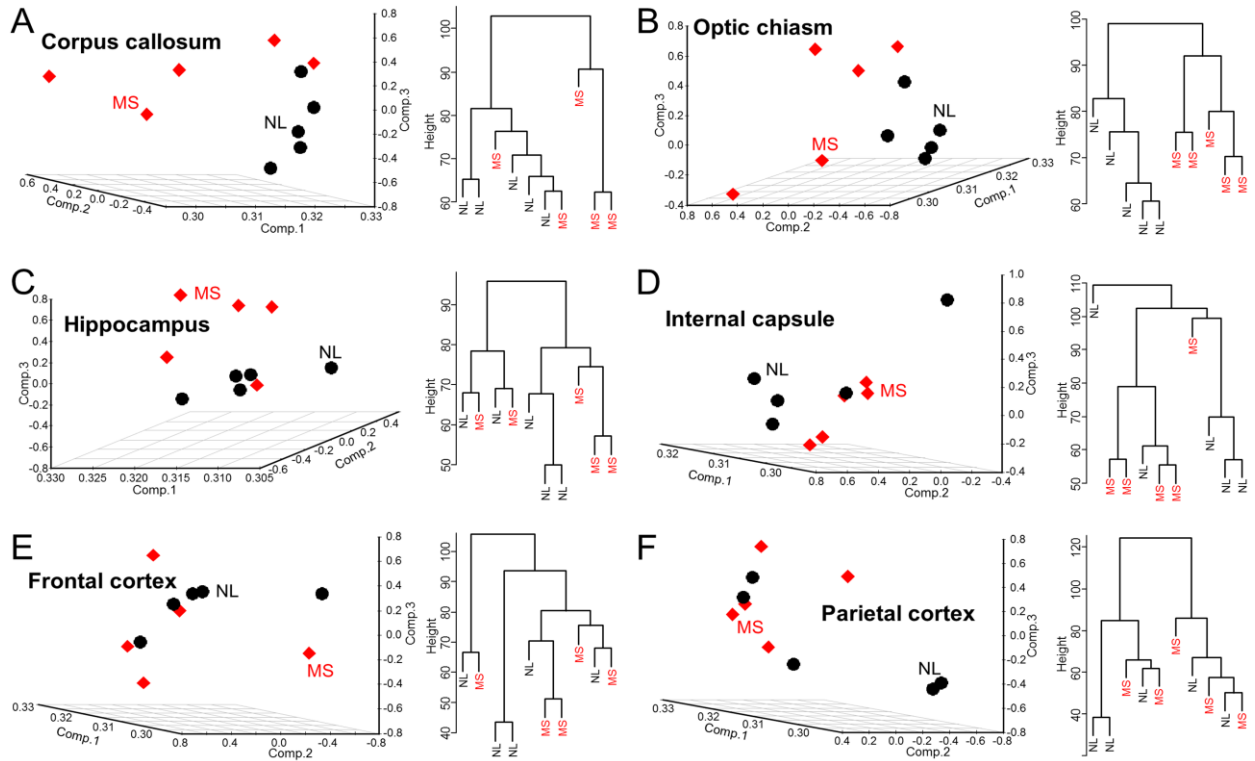


**Figure S1. Principal component analysis and hierarchical clustering of MS and NL samples from six different brain regions. Corpus callosum (A) and optic chiasm (B) showed the most separation between MS and NL as compared to the other four brain regions (C-F).**

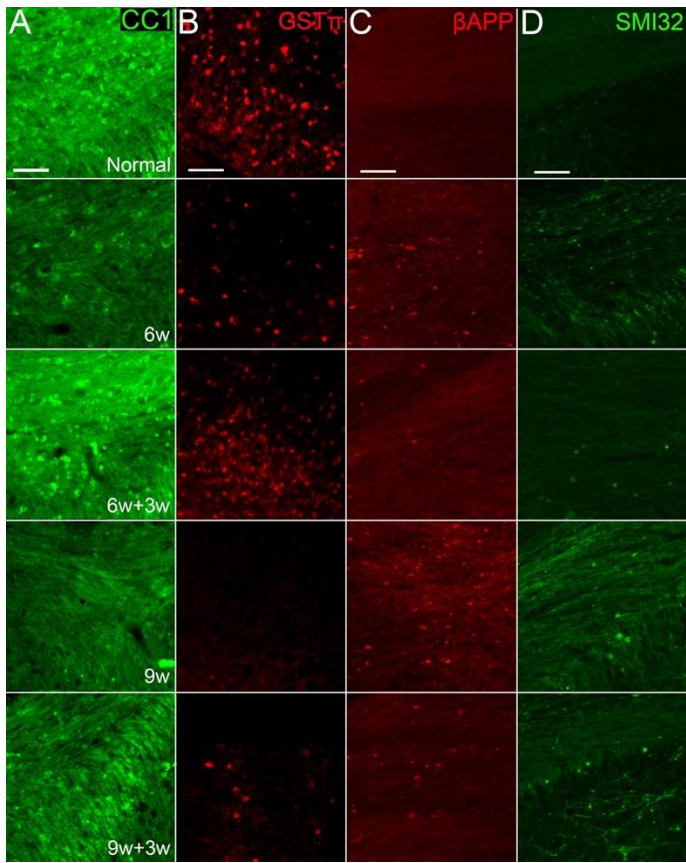


**Fig S2.** Representative images of corpus callosum sections stained for CC1 (A), GST $\pi$  (B),  $\beta$ APP (C), and SMI32 (D) in normal controls (Normal); mice fed with cuprizone diet for 6 weeks (6w); mice fed with cuprizone diet for 6 weeks then normal diet for 3 weeks (6w+3w), mice fed with cuprizone diet for 9 weeks (9w); and mice fed with cuprizone diet for 9 weeks then normal diet for 3 weeks (9w+3w). Quantitative analysis results are shown in Figure 3. Scale bar: 100 $\mu$ m.

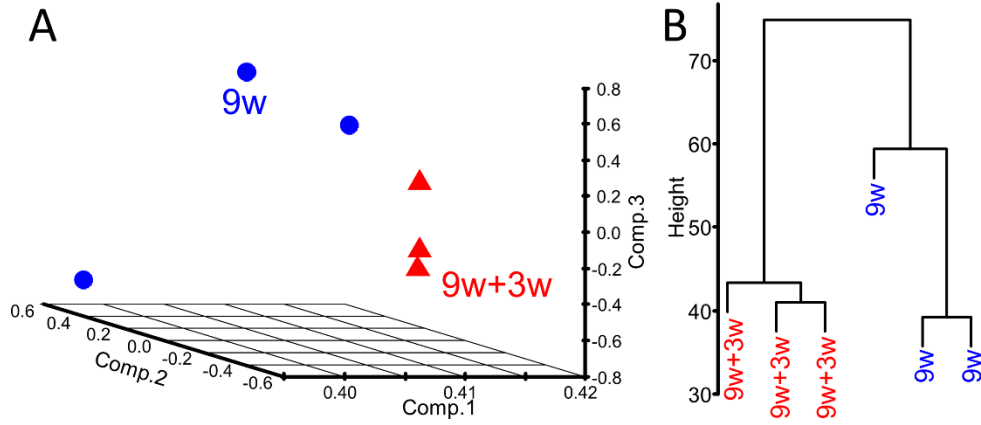


**Figure S3.** Principal component analysis (A) and hierarchical clustering (B) showed separation between groups during remyelination in mice fed with cuprizone for 9 weeks then normal diet for 3 weeks (9w+3w) versus mice fed with cuprizone diet for 9 weeks (9w).



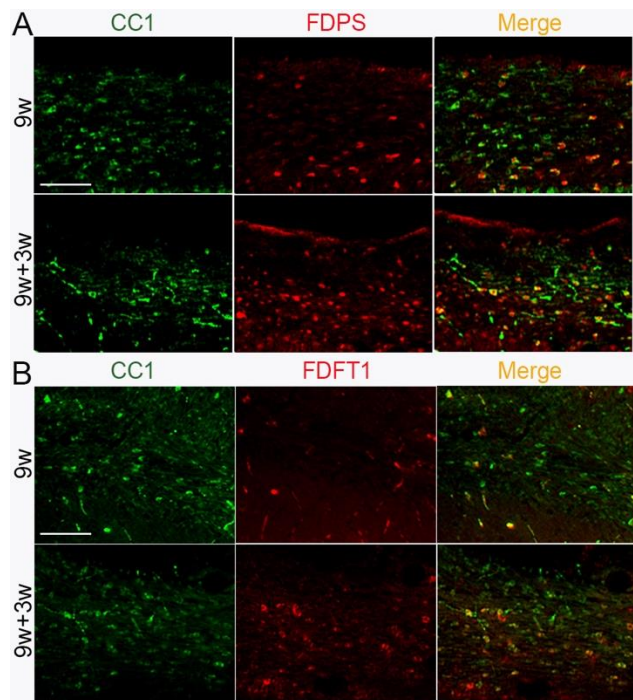


**Fig. S4. Validation of increased cholesterol synthesis gene expression in oligodendrocytes during remyelination.** Representative images of (A) FDPS (red) and (B) FDFT1 (red) co-stained with CC1 (green) in 9w mice and 9w+3w mice corpus callosum. Co-localization shown in Merge (yellow). Scale bar = 100 $\mu$ m.

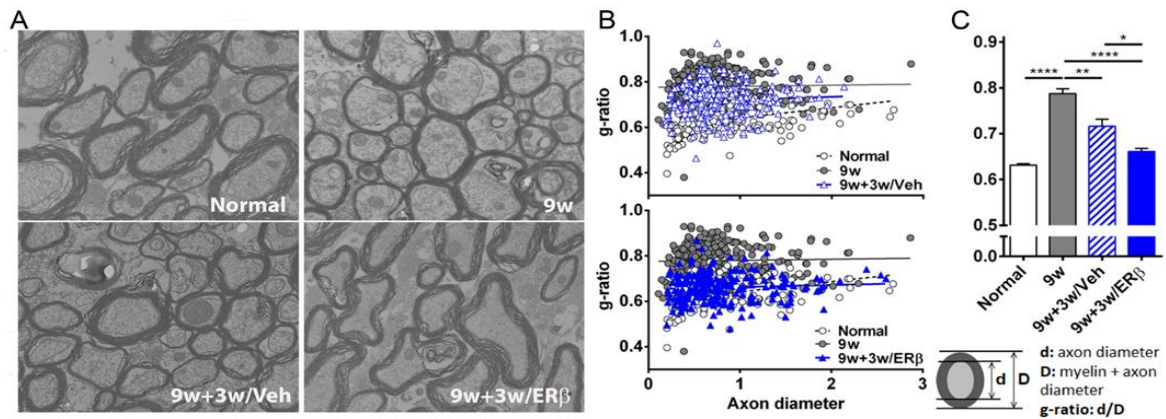


**Fig. S5. ER $\beta$ -ligand treatment during the remyelination phase of the cuprizone model further enhances remyelination.** (A) Representative electron microscopy images of ultra-resolution axons and myelin in the corpus callosum of normal controls (Normal); mice fed with cuprizone diet for 9 weeks (9w); mice fed with cuprizone for 9 weeks then normal diet for 3 weeks with vehicle treatment (9w+3w/Veh), and mice fed with cuprizone for 9 weeks then normal diet for 3 weeks with ER $\beta$  ligand treatment (9w+3w/Veh); Scale bar, 0.5 $\mu$ m. (B) Plots of g-ratio versus axon diameter for 9w+3w/Veh (top) and 9w+3w/ER $\beta$  (bottom) mice compared to 9w mice and normal controls (Normal), with a linear function. (C) Quantitative analysis showed that 9w mice had increased g-ratio compared to normal controls (Normal) indicative of demyelination. Vehicle treated mice after switch to normal diet (9w+3w/Veh) showed a decrease in g-ratio compared to 9w mice indicative of remyelination. ER $\beta$ -ligand treated (9w+3w/ER $\beta$ ) mice showed a further decrease in g-ratio compared to vehicle treated (9w+3w/Veh) indicative of enhanced remyelination.

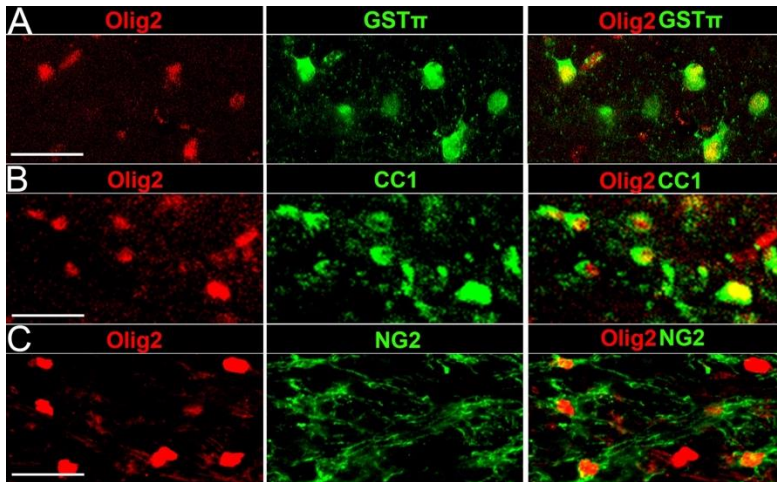


**Figure S6.** Representative images of double-labelling for GST $\pi$  (A), CC1 (B), or NG2 (C) with Olig2. Quantification analysis results are shown in Figure 8. Scale bar = 20 $\mu$ m.

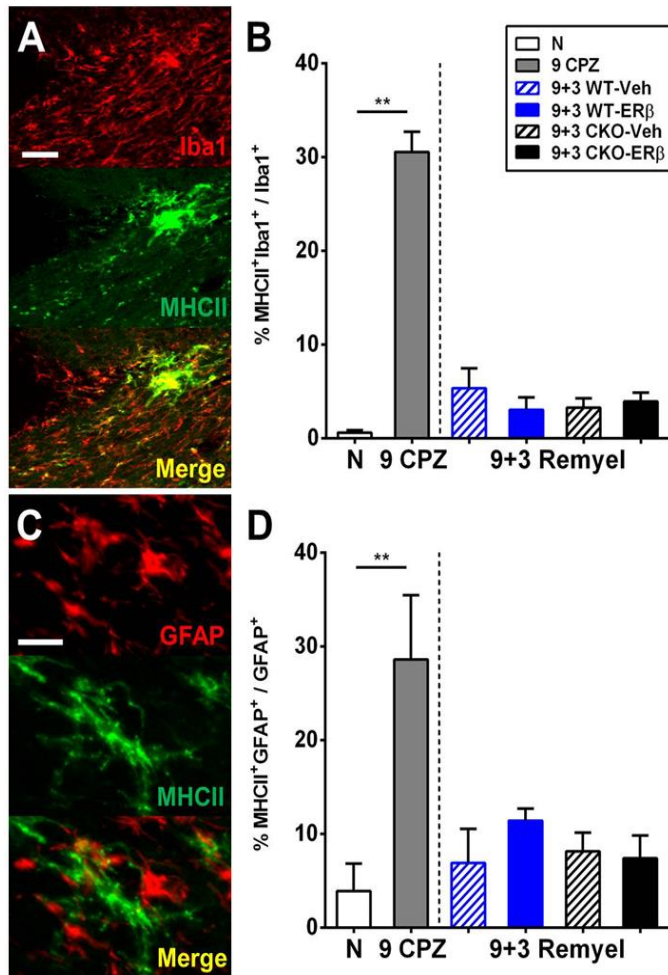


**Fig. S7. ER $\beta$ -ligand treatment had no effect on microglia and reactive astrocytes during remyelination.** (A) Representative images of Iba1 (red) microglia cells and MHCII (green) stained corpus callosum. Merged images show the co-localization of Iba1 and MHCII (yellow). Scale bar, 50  $\mu$ m (B) Quantitative analysis of MHCII+Iba1+ double positive among Iba1+ microglia cells. (C) Representative images of GFAP (red) reactive astrocytes and MHCII (green) stained corpus callosum. Merged images show the co-localization of GFAP and MHCII (yellow). Scale bar, 50  $\mu$ m (D) Quantitative analysis of MHCII+GFAP+ double positive among GFAP+ reactive astrocytes. \*\* $p < 0.01$ .

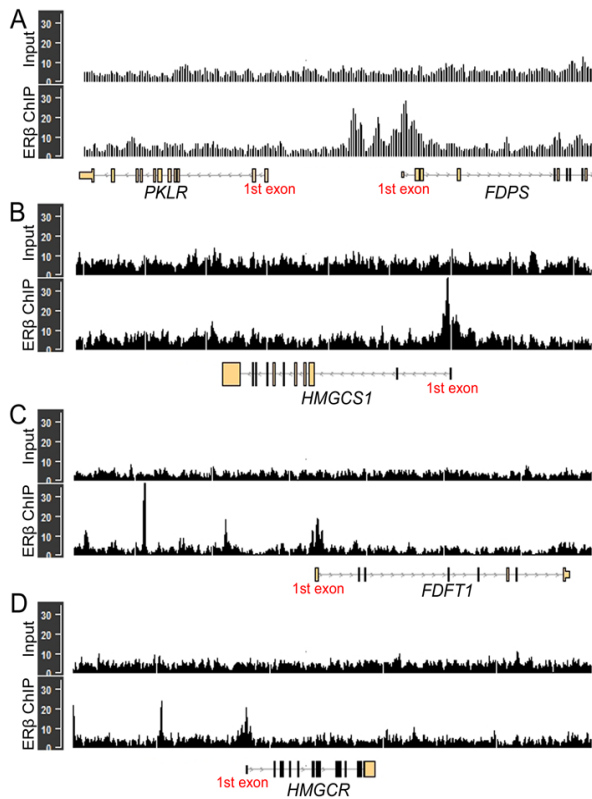


**Fig. S8. Human ER $\beta$  binding profiles for four cholesterol synthesis genes.**

ChIP-Seq data for doxycycline-inducible ER $\beta$  expressing human MDA-MB-231 cells treated with estradiol was obtained from GEO (GSE108981). For each genome region, the profiles for input and ChIP were listed as a comparison. Peaks in ER $\beta$  ChIP profiles indicate ER $\beta$  binding on those regions. **(A)** *FDPS*, **(B)** *HMGCS1*, **(C)** *FDFT1*, and **(D)** *HMGCR* had peaks around the 1<sup>st</sup> exons in ER $\beta$  ChIP profiles, while the negative control input profile (DNAs from chromatin before ChIP) did not show these peaks. As an additional negative control, the *PKLR* gene, near the *FDPS* gene, did not have a peak **(A)**.

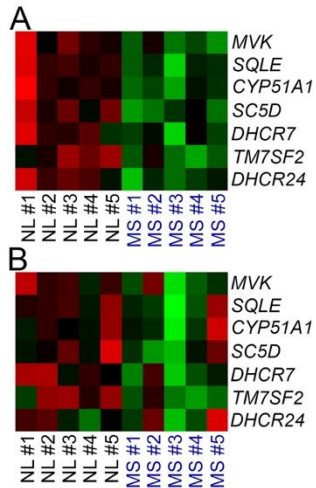


**Fig. S9. Cholesterol synthesis gene expression in optic chiasm and corpus callosum in MS and healthy control (NL) tissues.** (A) Heat maps of cholesterol synthesis pathway genes that were significantly different between MS and normal (NL) RNAs from optic chiasm (FDR < 0.1) (9) revealed that cholesterol synthesis pathway genes were decreased in MS (green). (B) The same set of cholesterol synthesis genes showed a trend of decrease in MS corpus callosum, but with more variability. Green color represents lower expression and red color represents higher expression. n = 10 human (5 MS, 5 normal).



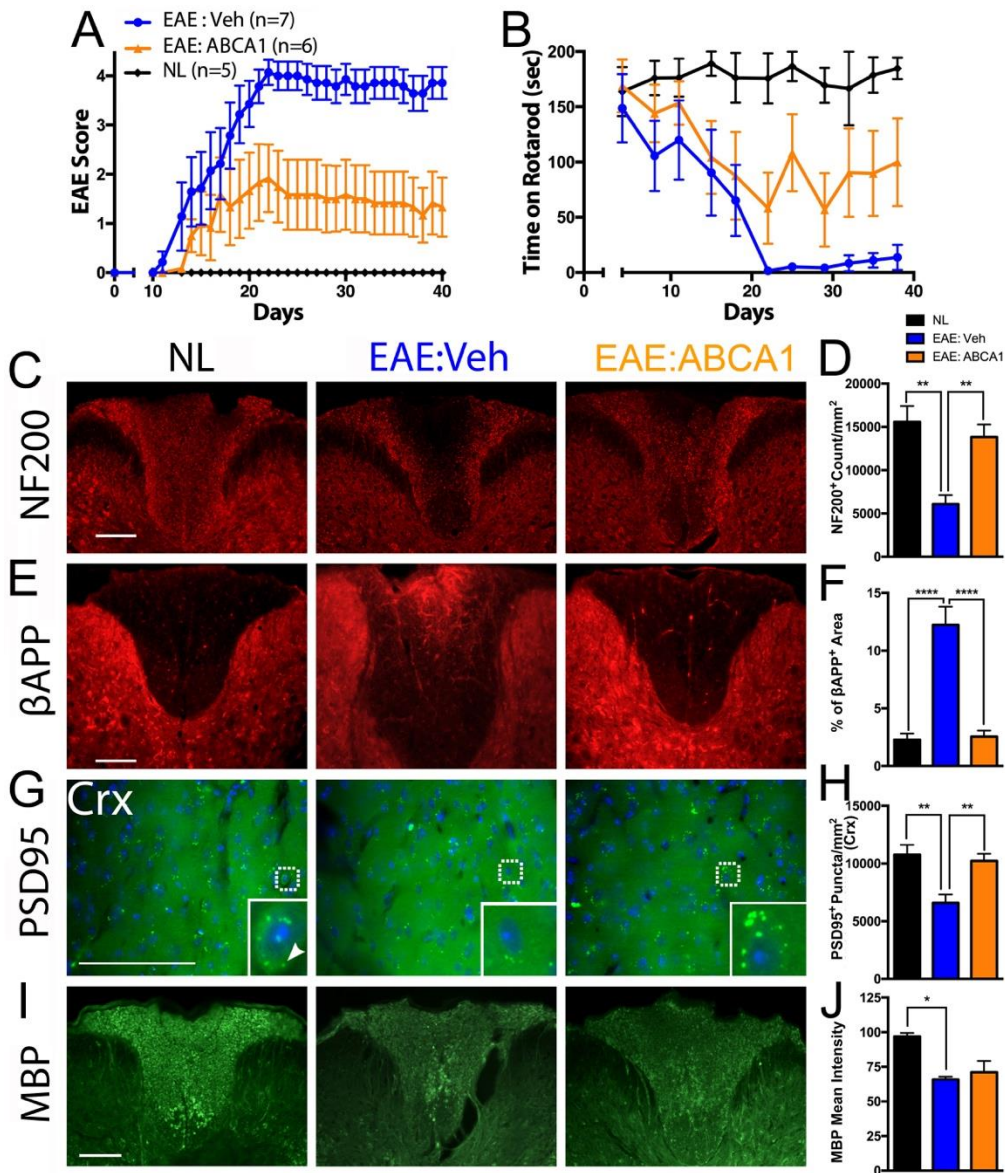


**Fig. S10. Treatment of EAE mice with ATP-binding cassette transporter A1 (ABCA1) agonist increases synapses and spares axons, but does not increase myelin staining.** Treatment with an ABCA1 agonist increased cholesterol synthesis gene expression in astrocytes (Itoh et al., 2018) and improved EAE outcomes. (A, B) EAE mice were treated with either vehicle (Veh, blue) or the ABCA1 agonist CS-6253 (30 mg/kg) (ABCA1, orange). (A) ABCA1 agonist treatment resulted in a reduction in standard EAE clinical severity scores

( $p < 0.0001$ ), and (B) an increase in the number of seconds mice stayed on the rotarod ( $p = 0.0077$ ), each as compared to vehicle treatment of EAE. (C-J) ABCA1 agonist treatment in EAE increased healthy axon numbers (increased NF200+ staining), decreased damaged axons (decreased  $\beta$ APP+ staining), increased synapses (PSD95+ puncta), but did not increase myelin intensity (MBP+ staining): (C) Representative 10x images of dorsal column in spinal cord with axons stained for NF200 (red), (E) axonal damage stained for beta-APP (red), (G) representative 40x image of post-synaptic protein stained for PSD95 in motor cortex, inset with white arrowhead indicating PSD95+ puncta, (I) representative 10x images of dorsal column spinal cord stained for MBP. Healthy control (NL), vehicle treated EAE (EAE:Veh), and ABCA1 agonist treated EAE (EAE:ABCA1). Scale bar = 100um. Quantitative analysis of each stain was shown in (D) NF200+ axonal count, (F) beta-APP+ percent area for axonal damage, (H) PSD95+ puncta densities in motor cortex, and (J) myelin staining intensity by MBP in dorsal column spinal cord. 4-7 mice were examined for each treatment group. p-values were determined by one-way ANOVA. Data are representative of two independent experiments. \* $p < 0.05$ , \*\* $p < 0.005$ , \*\*\*\* $p < 0.0001$ .



**Table S4. Cuprizone experiments in ER $\beta$ -ligand or vehicle treated Olig1-WT or Olig1-CKO.** Mean MBP intensity, mean difference, standard errors and significance levels for each comparison in all experiments. Repeated measures two-way ANOVA, with Bonferroni's multiple comparisons test. Wildtype mice that were vehicle treated (Veh WT) versus ER $\beta$  ligand treated (ER $\beta$  WT): conditional knockout mice that were vehicle treated (Veh CKO) versus ER $\beta$  ligand treated (ER $\beta$  CKO). 9w+3w indicates mice fed with cuprizone for 9 weeks followed by normal diet for 3 weeks; 9w+6w indicates mice fed with cuprizone for 9 weeks and normal diet for 6 weeks.

		MBP Mean intensity (Vehicle vs ER $\beta$ -ligand)						Mean Difference	Standard Error	p-value
Exp. 1	9w+3w	Veh WT	n=4	7.46	ER $\beta$ WT	n=10	10.3	-2.79	0.699	0.0047
		Veh CKO	n=4	7.8	ER $\beta$ CKO	n=5	7.24	0.56	0.932	> 0.9999
	9w+6w	Veh WT	n=5	9.26	ER $\beta$ WT	n=5	12.7	-3.42	1.082	0.0389
		Veh CKO	n=5	9.24	ER $\beta$ CKO	n=4	9.6	-0.36	1.148	> 0.9999
Exp. 2	9w+3w	Veh WT	n=5	11.7	ER $\beta$ WT	n=5	13.4	-1.679	0.284	0.0002
		Veh CKO	n=5	11.2	ER $\beta$ CKO	n=4	12	-0.859	0.302	0.0734
	9w+6w	Veh WT	n=4	13.9	ER $\beta$ WT	n=6	17.4	-3.497	0.777	0.0022
		Veh CKO	n=5	13.8	ER $\beta$ CKO	n=5	14.3	-0.463	0.762	> 0.9999
Exp. 3	9w+6w	Veh WT	n=4	15.4	ER $\beta$ WT	n=3	19.1	-3.762	1.082	0.0223
		Veh CKO	n=3	16.9	ER $\beta$ CKO	n=4	15.5	1.419	1.082	> 0.9999

**Table S5. Primer list for quantitative PCR**

<b>Gene</b>	<b>Forward Primer</b>	<b>Reverse Primer</b>
<i>Actβ</i>	GGCTCCTAGCACCATGAAGA	ACTCCTGCTTGCTGATCCAC
<i>Plp</i>	CCGACAAGTTTGTGGGCATC	TACATTCTGGCATCAGCGCA
<i>Ugt8a</i>	GCCGAAGGACGCGCTAT	CAAGGCCGATGCTAGTGTCT
<i>Pdgfra</i>	GTTGTGAGGCTGGTGGAGG	GTTGTGAGGCTGGTGGAGG
<i>Aldh1l1</i>	GGCTCCTAGCACCATGAAGA	ACTCCTGCTTGCTGATCCAC
<i>Syn</i>	GGGCCAATGATGGACTTCCT	GCCTGTCTCCTTGAACACGA
<i>Tmem119</i>	CTTCACCCAGAGCTGGTTCC	GGGAAGAGGCTGAAGAACCC
<i>Mbp</i>	GGAAGGCAGGTGATGGTTGA	ACACTGGAGGGCAAACACTC
<i>Mog</i>	TCCATCGGACTTTTGATCCTCA	GCTCCAGGAAGACACAACCA
<i>Mag</i>	GGTGTGAGGGAGGCAGTTG	CGTTGTCTGCTAGGCAAGCA
<i>Hmgcs1</i>	ATGGGGCTCGTGCATAGTAA	ACTCTCAGTGCTCCCCGTTA
<i>Fdps</i>	GCACTGACATCCAGGACAAC	AGCCACTTTTTCTGGGTCTCT
<i>Fdft1</i>	TCCCTGACGTCCTCACCTAC	CCCCTTCCGAATCTTCACTA

**Table S6. Antibody list for immunofluorescence.**

<b>Antibody</b>	<b>Dilution factor</b>	<b>Catalog# and company</b>
anti-HA	1:500	16B12, Biolegend
anti-HA	1:1000	MA5-27915, Thermo Fisher Scientific
anti-GST $\pi$	1:1000	ADI-MSA-102, Enzo Life Sciences
anti-GFP	1: 200	A-11120, Thermo Fisher Scientific
anti-GFAP	1:1000	Z0334, Dako
anti-NF200	1:750	N4142, Sigma
anti-Iba1	1:10,000	Wako Chemicals
anti-MBP	1:750	MAB386, EMD Millipore
anti-CC1	1:500	OP80, Calbiochem
anti- $\beta$ APP	1:200	51-2700, Thermo Fisher Scientific
anti-SMI32	1:1000	NE1023, EMD Millipore
anti-HMGCS1	1:500	PA5-29488, ThermoFisher Scientific
anti-FDPS	1:500	Biolegend
anti-FDFT1	1:500	ab109723, Abcam
anti-MHCII (I-A/I-E)	1:400	M5/114.15.2, Biolegend
anti-Olig2	1:1000	AB9610, EMD Millipore
anti-Olig2	1:200	MABN50, EMD Millipore
anti-NG2	1:500	AB5320 EMD Millipore
anti-rabbit-Cy <sup>TM</sup> 5	1:1000	111-175-144, Jackson Immunoresearch
anti-rabbit-Cy3	1:1000	AP132C, EMD Millipore
anti-rabbit-DyLight <sup>®</sup> 649	1:1000	AP187SD, EMD Millipore

anti-rat-Cy3	1:1000	AP136C, EMD Millipore
anti-rat-Cy5	1:1000	AB6565, Abcam
anti-mouse-Alexa Fluor® 488	1:1000	115-545-166, Jackson ImmunoResearch
anti-mouse- DyLight®649	1:1000	AP181SD, EMD Millipore

## Additional data

**Table S1.** Human differentially expressed gene list in MS vs NL (excel)

**Table S2.** Cell marker gene list for seven CNS cell types (excel)

**Table S3.** Differentially expressed genes in oligodendrocytes during remyelination (excel)

## References in Supplemental Information

1. Bolger AM, Lohse M, & Usadel B (2014) Trimmomatic: a flexible trimmer for Illumina sequence data. *Bioinformatics* 30(15):2114-2120.
2. Gaidatzis D, Lerch A, Hahne F, & Stadler MB (2015) QuasR: quantification and annotation of short reads in R. *Bioinformatics* 31(7):1130-1132.
3. Robinson MD, McCarthy DJ, & Smyth GK (2010) edgeR: a Bioconductor package for differential expression analysis of digital gene expression data. *Bioinformatics* 26(1):139-140.
4. Zhang Y, *et al.* (2014) An RNA-sequencing transcriptome and splicing database of glia, neurons, and vascular cells of the cerebral cortex. *J Neurosci* 34(36):11929-11947.
5. Sanz E, *et al.* (2009) Cell-type-specific isolation of ribosome-associated mRNA from complex tissues. *Proc Natl Acad Sci U S A* 106(33):13939-13944.
6. Lu QR, *et al.* (2002) Common developmental requirement for Olig function indicates a motor neuron/oligodendrocyte connection. *Cell* 109(1):75-86.

7. Kim RY, *et al.* (2018) Oestrogen receptor beta ligand acts on CD11c+ cells to mediate protection in experimental autoimmune encephalomyelitis. *Brain* 141(1):132-147.
8. Mei F, *et al.* (2016) Accelerated remyelination during inflammatory demyelination prevents axonal loss and improves functional recovery. *Elife* 5.
9. Itoh N, *et al.* (2018) Cell-specific and region-specific transcriptomics in the multiple sclerosis model: Focus on astrocytes. *Proc Natl Acad Sci U S A* 115(2):E302-E309.
10. Anderson MA, *et al.* (2016) Astrocyte scar formation aids central nervous system axon regeneration. *Nature* 532(7598):195-200.
11. Reese JM, *et al.* (2018) ERbeta-mediated induction of cystatins results in suppression of TGFbeta signaling and inhibition of triple-negative breast cancer metastasis. *Proc Natl Acad Sci U S A* 115(41):E9580-E9589.
12. Lawrence M, *et al.* (2013) Software for computing and annotating genomic ranges. *PLoS Comput Biol* 9(8):e1003118.
13. Hahne F & Ivanek R (2016) Visualizing Genomic Data Using Gviz and Bioconductor. *Methods Mol Biol* 1418:335-351.
14. Verity AN, Bredesen D, Vonderscher C, Handley VW, & Campagnoni AT (1993) Expression of myelin protein genes and other myelin components in an oligodendrocytic cell line conditionally immortalized with a temperature-sensitive retrovirus. *J Neurochem* 60(2):577-587.

15. Bourdeau V, *et al.* (2004) Genome-wide identification of high-affinity estrogen response elements in human and mouse. *Mol Endocrinol* 18(6):1411-1427.